
On Exact Bit-level Reversible Transformers Without Changing Architectures

Guoqiang Zhang
University of Exeter
g.z.zhang@exeter.ac.uk

J.P. Lewis
NVIDIA
jpl@nvidia.com

W. Bastiaan Kleijn
Victoria University of Wellington
bastiaan.kleijn@vuw.ac.nz

Abstract

In the literature, various reversible deep neural networks (DNN) models have been proposed to reduce memory consumption or improve data-throughput in the training process. However, almost all existing reversible DNNs either are constrained to have special structures or are constructed by modifying the original DNN architectures considerably to enable reversibility. In this work, we propose exact bit-level reversible transformers¹ without changing the architectures in the inference procedure. The basic idea is to first treat each transformer block as the Euler integration approximation for solving an ordinary differential equation (ODE) and then incorporate the technique of bidirectional integration approximation (BDIA) (see [26] for BDIA-based diffusion inversion) into the neural architecture together with activation quantization to make it exactly bit-level reversible, referred to as BDIA-transformer. In the training process, we let a hyper-parameter γ in BDIA-transformer randomly take one of the two values $\{0.5, -0.5\}$ per transformer block for averaging two consecutive integration approximations, which regularizes the models for improving the validation accuracy. Light-weight side information per transformer block is required to be stored in the forward process to account for binary quantization loss to enable exact bit-level reversibility. In the inference procedure, the expectation $\mathbb{E}(\gamma) = 0$ is taken to make the resulting architectures of BDIA-transformer be identical to transformers up to activation quantization. Empirical study indicates that BDIA-transformers outperform their original counterparts notably due to the regularization effect of the γ parameter.

1 Introduction

Nowadays, one active research trend in deep learning intends to scale up the size of both the deep neural networks (DNNs) and training data, aiming to obtain universal machine-learning models that are capable of accomplishing various tasks. One typical example is the large language models (LLMs) such as GPT-4 [1] and Llama 2 [20] that can, for example, have informative and friendly conversations with humans, solve mathematical problems, or produce high-quality source codes for programming tasks. One main bottleneck for training those large DNNs is that they often require large on-chip memory and large inter-chip communication bandwidth across many chips

¹In fact, by following the same principle in this paper, we can also design exact bit-level reversible ResNet without changing its architecture in the inference procedure. We focus on transformer in this paper due to its popularity in the field of generative artificial intelligence (AI).

to accommodate both the DNN model and the intermediate activations of the input data-batch in back-propagation [8], which is referred to as *memory wall* in the literature.

One promising technique to alleviate the issue of memory wall is to design and train reversible DNNs [5; 6; 2; 15]. By doing so, the intermediate activations in the forward pass do not have to be stored in the memory to allow for back-propagation. Instead, they can be recomputed on-the-fly in backward pass by exploiting the reversibility of the DNN to save the memory consumption to a large margin when the DNN is considerably deep. The procedure essentially reduces memory consumption at the cost of extra reasonable amount of computation.

In particular, the so-called NICE and Real NV reversible transformation models were first proposed in [5] and [6], respectively. Inspired by the NICE and Real NV formulations, more advanced reversible residual models have been proposed later on, which includes, for example, RevNet [9], Glow [13], i-RevNet [12], i-ResNet [2], layerwise inversion [11], Fourier-transformation based CNN inversion [7], Mintnet [18], and normalizing flow [14]. Another line of research work enforces reversibility in deep learning from the perspective of ordinary differential equations (ODEs), which includes FFJORD [10], leapfrog network [3], neural ODEs [4], momentum residual networks [16], and neural ODE inversion [19].

Recently, the research on reversability has been switched to other types of neural networks. The authors in [15; 28] proposed reversible vision transformers due to the popularity of LLMs. The work [21] utilized a reversible diffusion sampling method to optimize the noisy representation for the task of diffusion based image editing. To our best knowledge, all the above existing reversible DNNs either are constrained to have special structures or are constructed by modifying the original DNN architectures considerably to enable reversibility.

In this paper, we design a new type of reversible transformers without changing the architectures in the inference procedure by utilizing the technique of bidirection integration approximation (BDIA). BDIA was recently proposed in [26] to enable diffusion inversion for round-trip image editing without the need for retraining diffusion models. To be able to incorporate BDIA into transformers for online back-propagation, we follow the common practice by treating each transformer block as the Euler integration approximation for solving an ordinary differential equation (ODE).

We make two main contributions in this work. Firstly, we propose BDIA-transformers by introducing a random hyper-parameter $\gamma \in \{-0.5, 0.5\}$ per transformer block per training sample to regularize the DNN models for performance improvement. The γ parameter essentially intends to average two consecutive integration approximations. In the inference procedure, The expectation $\mathbb{E}[\gamma] = 0$ is utilized, which makes the architectures of BDIA-transformers reduce to the original transformers. Therefore, our proposed method for enforcing reversibility is more flexible than existing ones.

Secondly, we perform activation quantization to allow for exact bit-level reversibility of BDIA-transformers. We note that the special setup of the γ values in the subset $\in \{-0.5, 0.5\}$ when performing activation quantization leads to 1-bit information loss per activation value per transformer block. Therefore, light-weight side information per transformer block needs to be stored in the training process to account for the above 1-bit information loss. Experimental results on ViT and NanoGPT demonstrate the effectiveness of the BDIA technique when training transformers.

2 Related Works

In recent years, various quantization strategies [24; 23; 22] have been proposed in the training and/or inference processes of DNN models over low-precision devices. For instance, the work [23] successfully performed quantization on DNN weights, activations, gradients and errors in the training and inference processes and obtained promising results. In summary, it is found in the literature that the obtained validation performance after applying those quantization operations in the DNN models is competitive to the original ones. In our work, we only need to apply activation quantity to enable exact bit-level reversibility in training BDIA-transformers.

3 Preliminary

Diffusion sampling via solving ODE: Recently, the work [26] proposed the BDIA technique to enable diffusion inversion for effective round-trip image editing. From a high level point of view,

BDIA can be viewed as a time-reversible ODE solver. Suppose the initial diffusion state \mathbf{z}_T at time step T is sampled from a Gaussian distribution $\mathcal{N}(0, \sigma_T^2)$. The diffusion-based sampling process for generating realist images \mathbf{z}_ϵ at time $t = \epsilon > 0$ can be realized by solving a probability ordinary differential equation (ODE)

$$d\mathbf{z} = \mathbf{d}(\mathbf{z}, t)dt = \mathbf{d}(\mathbf{z}, t)dt \quad (1)$$

over the time interval $t \in [T, \epsilon]$. The gradient vector $\mathbf{d}(\mathbf{z}, t)$ includes the output of a pre-trained DNN model with (\mathbf{z}_t, t) as its input. The common practice for solving the above ODE is to first discretize the continuous time interval $[T, \epsilon]$ properly into a set of timesteps $\{t_i | i = 0, \dots, N\}$ with $t_0 = T$ and $t_N = \epsilon$, and then perform certain integration approximation per small time-interval sequentially to compute the final diffusion state $\mathbf{z}_N = \mathbf{z}_\epsilon$.

BDIA: Suppose we would like to estimate the next diffusion state $\mathbf{z}_{i+1} = \mathbf{z}_{t_{i+1}}$ by solving (1) based on the recent information (\mathbf{z}_i, t_i) and $(\mathbf{z}_{i-1}, t_{i-1})$, where $\mathbf{z}_j = \mathbf{z}_{t_j}$ for $j = i - 1, i$. The basic idea of BDIA is to compute \mathbf{z}_{i+1} by performing both the forward integration approximation $\Delta(t_i \rightarrow t_{i+1} | \mathbf{z}_i)$ ($\approx \int_{t_i}^{t_{i+1}} \mathbf{d}(\mathbf{z}, t)dt$) and the backward integration approximation $\Delta(t_i \rightarrow t_{i-1} | \mathbf{z}_i)$ ($\approx -\int_{t_{i-1}}^{t_i} \mathbf{d}(\mathbf{z}, t)dt$) conditioned on \mathbf{z}_i . One popular method for implementing $\Delta(t_i \rightarrow t_{i+1} | \mathbf{z}_i)$ and $\Delta(t_i \rightarrow t_{i-1} | \mathbf{z}_i)$ in the literature of diffusion models is by employing the DDIM update expression (see [17; 27; 26] for details). With the above two integration approximations, \mathbf{z}_{i+1} can be expressed as

$$\mathbf{z}_{i+1} = \mathbf{z}_{i-1} - \underbrace{(1 - \gamma)(\mathbf{z}_{i-1} - \mathbf{z}_i) - \gamma \Delta(t_i \rightarrow t_{i-1} | \mathbf{z}_i)}_{\approx \int_{t_{i-1}}^{t_i} \mathbf{d}(\mathbf{z}, t)dt} + \underbrace{\Delta(t_i \rightarrow t_{i+1} | \mathbf{z}_i)}_{\approx \int_{t_i}^{t_{i+1}} \mathbf{d}(\mathbf{z}, t)dt} \quad (2)$$

$$= \gamma \mathbf{z}_{i-1} + (1 - \gamma) \mathbf{z}_i - \gamma \Delta(t_i \rightarrow t_{i-1} | \mathbf{z}_i) + \Delta(t_i \rightarrow t_{i+1} | \mathbf{z}_i), \quad (3)$$

where $\gamma \in (0, 1]$ averages $\Delta(t_i \rightarrow t_{i-1} | \mathbf{z}_i)$ and $(\mathbf{z}_{i-1} - \mathbf{z}_i)$ for the time-slot $[t_{i-1}, t_i]$. The minus sign in front of the two quantities are due to the reverse integration direction. The quantity $-(\mathbf{z}_{i-1} - \mathbf{z}_i)$ can be taken as the integration approximation for $\int_{t_{i-1}}^{t_i} \mathbf{d}(\mathbf{z}, t)dt$ computed earlier. We note that negative γ values are not applicable to the diffusion models considered in [26].

On reversibility of BDIA:

The update expression (3) is carefully designed in [26] to enable diffusion inversion for round-trip image editing. By reformulating (3), \mathbf{z}_{i-1} can be easily computed in terms of $(\mathbf{z}_i, \mathbf{z}_{i+1})$. We note that due to the nature of float-point datatype, there might be error accumulation in round-trip image reconstruction, where the corresponding diffusion states in the forward and reverse process are not identical. In practice, error accumulation of BDIA in diffusion inversion is not a big issue [26] due to the fact that the number of timesteps is generally set to be small (e.g., 50 timesteps in either forward or reverse process) to make the time complexity reasonable.

One main difference between diffusion inversion and reversible Transformers is that no gradient is needed to be back-propagated in diffusion inversion for updating the DNN model. As a result, even if there is error accumulation in diffusion inversion, it is less severe than in reversible transformers where error accumulation in online back-propagation would slow down the training speed or even make the training fail especially for very deep models like LLMs. In next section, we will explain how to design exact bit-level reversible transformers in the training process to avoid any error-accumulation while at the same time, maintains the architectures of the transformer in the inference procedure.

4 Exact Bit-Level Reversible Transformers via BDIA

In this section, we first briefly review the transformer update expressions from the ODE viewpoint. We then propose the BDIA-transformer that enable exact bit-level reversibility with activation quantization. Specially, we will study the impact of the two γ values $\{-0.5, -0.5\}$ in BDIA-transformer. In addition, we explain why additional light-weight side-information is required to be stored to account for the binary quantization loss.

4.1 Revisiting transformer update expression

A typical transformer block consists of the attention function (denoted as $\mathbf{f}(\cdot)$) and the function of feed-forward network (FFN) (denoted as $\mathbf{g}(\cdot)$), of which the trainable parameters are generally different for different block indices. Accordingly, the output \mathbf{x}_{k+1} of the k th transformer block can be mathematically represented in terms of the input \mathbf{x}_k as

$$\mathbf{x}_{k+1} = \mathbf{x}_k + \underbrace{\mathbf{f}_k(\mathbf{x}_k) + \mathbf{g}_k(\mathbf{x}_k + \mathbf{f}_k(\mathbf{x}_k))}_{\mathbf{h}_k(\mathbf{x}_k)}, \quad (4)$$

which involves two residual connections. For simplicity, we ignore the pre-normalisation operations in (4), which in fact does not affect the design of BDI-transformers later on.

It is well known from the literature [4] that the k th forward step in (4) can be viewed as the Euler integration approximation of an ODE at timestep t_k :

$$\begin{aligned} \mathbf{x}_{k+1} = \mathbf{x}_k + \mathbf{h}_k(\mathbf{x}_k) &= \mathbf{x}_k + \overbrace{\tilde{\mathbf{d}}(\mathbf{x}_k, t_k)(t_{k+1} - t_k)}^{\Delta(t_k \rightarrow t_{k+1} | \mathbf{x}_k)} \\ &\approx \mathbf{x}_k + \int_{t_k}^{t_{k+1}} \tilde{\mathbf{d}}(\mathbf{x}, t) dt, \end{aligned} \quad (5)$$

where $\tilde{\mathbf{d}}(\mathbf{x}_k, t_k)$ denotes the gradient vector with (\mathbf{x}_k, t_k) as the input. Both $\tilde{\mathbf{d}}(\mathbf{x}_k, t_k)$ and $(t_{k+1} - t_k)$ are implicitly learned via the composite function $\mathbf{h}_k(\mathbf{x}_k)$, which is alternatively denoted as $\Delta(t_k \rightarrow t_{k+1} | \mathbf{x}_k)$.

4.2 BDIA-transformer without quantization

In this subsection, we first derive the update expressions of BDIA-transformer without quantization, and then study the impact of the γ values in $\{0.5, -0.5\}$. When $k = 0$, \mathbf{x}_1 can be computed as

$$\mathbf{x}_1 = \mathbf{x}_0 + \mathbf{h}_0(\mathbf{x}_0) = \mathbf{x}_0 + \Delta(t_0 \rightarrow t_1 | \mathbf{x}_0), \quad (6)$$

The update expression for \mathbf{x}_{k+1} in the training process, $N - 1 \geq k \geq 1$, can be obtained by utilizing (2)-(3). In particular, we let

$$\Delta(t_k \rightarrow t_{k-1} | \mathbf{x}_k) = -\mathbf{h}_k(\mathbf{x}_k) \quad (7)$$

$$\Delta(t_k \rightarrow t_{k+1} | \mathbf{x}_k) = \mathbf{h}_k(\mathbf{x}_k). \quad (8)$$

By combining (7)-(8) and (2)-(3) with $i = k$, the update expression \mathbf{x}_{k+1} , $N - 1 \geq k \geq 1$, can be represented as

$$\mathbf{x}_{k+1} = \mathbf{x}_{k-1} + (1 - \gamma)(\mathbf{x}_k - \mathbf{x}_{k-1}) + (1 + \gamma)\mathbf{h}_k(\mathbf{x}_k), \quad (9)$$

$$= \gamma\mathbf{x}_{k-1} + (1 - \gamma)\mathbf{x}_k + (1 + \gamma)\mathbf{h}_k(\mathbf{x}_k), \quad (10)$$

where in general, γ is recommended to be randomly selected from $\{0.5, -0.5\}$ with equal probability per training sample per transform block. This is different from the work of BDIA-based diffusion inversion [26] where γ has to be positive.

In the inference stage, $\mathbb{E}(\gamma) = 0$ is taken to replace γ in (10), which leads to a simpler update expression that only involves $(\mathbf{x}_k, \mathbf{x}_{k+1})$:

$$\mathbf{x}_{k+1} = \mathbf{x}_k + \mathbf{h}_k(\mathbf{x}_k), \quad (11)$$

which is identical to the original transformer update expression (4).

Impact of γ parameter: We now study the impact of the γ parameter in (10). When $\gamma = 0.5$, it follows from (2)-(3) and (7)-(8) that

$$\int_{t_{k-1}}^{t_k} \tilde{\mathbf{d}}(\mathbf{x}_\tau, \tau) d\tau \approx 0.5(\mathbf{x}_k - \mathbf{x}_{k-1}) + 0.5\mathbf{h}_k(\mathbf{x}_k) \quad (12)$$

$$\int_{t_k}^{t_{k+1}} \tilde{\mathbf{d}}(\mathbf{x}_\tau, \tau) d\tau \approx \mathbf{h}_k(\mathbf{x}_k). \quad (13)$$

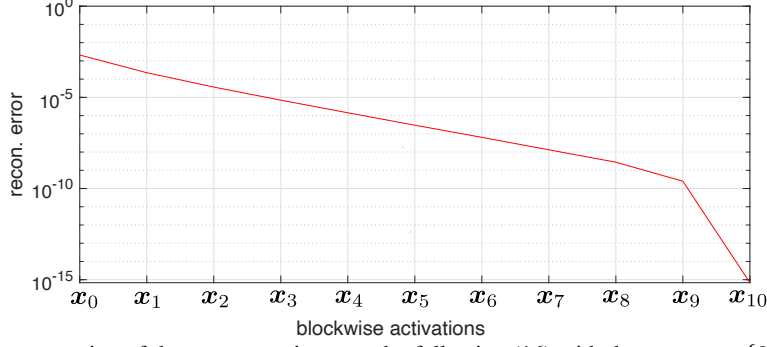


Figure 1: Demonstration of the reconstruction error by following (16) with the setup $\gamma \in \{0.5, -0.5\}$ when training GPT2 with 12 transformer blocks.

The expression (12) indicates that the function $\mathbf{h}_k(\mathbf{x}_k)$ partially plays the role of $(\mathbf{x}_k - \mathbf{x}_{k-1})$ for the time interval $[t_{k-1}, t_k]$.

When $\gamma = -0.5$, the two integrations $\int_{t_{k-1}}^{t_k} \tilde{\mathbf{d}}(\mathbf{x}_\tau, \tau) d\tau$ and $\int_{t_k}^{t_{k+1}} \tilde{\mathbf{d}}(\mathbf{x}_\tau, \tau) d\tau$ are approximated differently, given by

$$\int_{t_{k-1}}^{t_k} \tilde{\mathbf{d}}(\mathbf{x}_\tau, \tau) d\tau \approx (\mathbf{x}_k - \mathbf{x}_{k-1}) \quad (14)$$

$$\int_{t_k}^{t_{k+1}} \tilde{\mathbf{d}}(\mathbf{x}_\tau, \tau) d\tau \approx 0.5\mathbf{h}_k(\mathbf{x}_k) + 0.5(\mathbf{x}_k - \mathbf{x}_{k-1}). \quad (15)$$

As indicated in (15), the integration $\int_{t_k}^{t_{k+1}} \tilde{\mathbf{d}}(\mathbf{x}, t) dt$ when computing \mathbf{x}_{k+1} is approximated by the weighted average of $(\mathbf{x}_k - \mathbf{x}_{k-1})$ and $\mathbf{h}_k(\mathbf{x}_k)$. In this case, the function $(\mathbf{x}_k - \mathbf{x}_{k-1})$ partially plays the role of $\mathbf{h}_k(\mathbf{x}_k)$ for the time interval $[t_k, t_{k+1}]$.

The above analysis indicates that the γ parameter can work as a regularizer when training the BDIA-transformer. One can treat the γ parameter as a random variable that can take values in $\{0.5, -0.5\}$ with equal probability in the training process. The purpose for doing so is to make the neighbouring transformer blocks to smoothly change along with the increasing block index. The setup of $\mathbb{E}[\gamma] = 0$ can then be used in the inference stage.

Remark 1. *If reversibility is not of concern at all, one can freely specify the values for the random variable γ in the training process as long as its distribution is symmetric around 0 such that $\mathbb{E}[\gamma] = 0$ for maintaining the original DNN architectures in the inference procedure.*

4.3 On exact bit-level reversibility of BDIA-transformer with quantization

As explained in Section 1, one strategy for reducing memory consumption in training DNN models like LLMs is to perform online back-propagation. That is, the intermediate activation outputs from the top neural block until the bottom one are computed online when performing back-propagation to update the DNN model. In this subsection, we first discuss the reversibility issue of the update expression (10). We then consider performing activation quantization to enable exact bit-level reversibility. We note that light-weight side information is required to be stored per transformer block for lossless online back-propagation.

Limitation of the reversibility of (10): The update expression (10) is theoretically reversible. That is, \mathbf{x}_{k-1} can be computed in terms of $(\mathbf{x}_k, \mathbf{x}_{k+1})$ as

$$\mathbf{x}_{k-1} = \mathbf{x}_{k+1}/\gamma - (1 - \gamma)/\gamma \mathbf{x}_k - (1 + \gamma)/\gamma \mathbf{h}_k(\mathbf{x}_k). \quad (16)$$

However, in practice, the setup $\gamma \in \{0.5, -0.5\}$ would lead to non-negligible accumulation error especially for very deep DNN models. The factor $\frac{1}{\gamma} = \pm 2$ in front of \mathbf{x}_{k+1} would amplify the error when k decreases from $N - 1$ to 1, making the online back-propagation unstable. Fig. 1 illustrates that the reconstruction error indeed increases when applying the online-back-propagation from the top block until the bottom one.

BDIA-transformer with quantization: To allow for lossless online back-propagation, we propose to perform activation quantization. In particular, we use $\mathcal{Q}_l[\cdot]$ to denote the quantization operation

to the bit-level precision of 2^{-l} :

$$\mathcal{Q}_l[y] = \text{round}[y/2^{-l}]2^{-l}. \quad (17)$$

Upon introducing $\mathcal{Q}_l[\cdot]$, the new update expression for BDIA-transformer can be represented as

$$\mathbf{x}_0 \leftarrow \mathcal{Q}_l[\mathbf{x}_0], \quad (18)$$

$$\mathbf{x}_1 = \mathbf{x}_0 + \mathcal{Q}_l[\mathbf{h}_0(\mathbf{x}_0)] \quad (19)$$

$$s_{k-1}[m] = \begin{cases} 1 & \text{if } \text{mod}(\mathbf{x}_{k-1}[m]/2^{-l}, 2) = 1 \\ 0 & \text{otherwise} \end{cases} \quad k \geq 1 \quad (20)$$

$$\mathbf{x}_{k+1} = \mathcal{Q}_l[\gamma(\mathbf{x}_{k-1} + s_{k-1}2^{-l})] + \mathcal{Q}_l[(1 - \gamma)\mathbf{x}_k + (1 + \gamma)\mathbf{h}_k(\mathbf{x}_k)] \quad k \geq 1, \quad (21)$$

where $\gamma \in \{0.5, -0.5\}$, $\mathbf{x}_{k-1}[m]$ denotes the m th element of \mathbf{x}_{k-1} . The m th element $s_{k-1}[m]$ indicates if the integer value $\mathbf{x}_{k-1}[m]/2^{-l}$ is odd or not. It is immediate from (18)-(21) that $\mathbf{x}_k = \mathcal{Q}_l[\mathbf{x}_k]$ for all $N \geq k \geq 0$. That is, all the intermediate activation outputs $\{\mathbf{x}_k\}_{k=0}^N$ have fix-point precision of 2^{-l} .

Again in the inference procedure, we replace γ in (21) by $\mathbb{E}(\gamma) = 0$. As a result, the update expression (21) can be simplified to be

$$\mathbf{x}_{k+1} = \mathcal{Q}_l[\mathbf{x}_k + \mathbf{h}_k(\mathbf{x}_k)] \quad k \geq 1. \quad (22)$$

The only difference of (22) w.r.t. the original transformer update expression (4) is that the quantization operation $\mathcal{Q}_l[\cdot]$ is performed for each activation output.

On reversibility of (21) by storing light-weight side information: We now consider recovering \mathbf{x}_{k-1} from $(\mathbf{x}_k, \mathbf{x}_{k+1})$ by utilizing (20)-(21). By using the fact that $\gamma \in \{0.5, -0.5\}$ and the definition for s_{k-1} , we can easily conclude that the quantity $\mathcal{Q}_l[\gamma(\mathbf{x}_{k-1} + s_{k-1}2^{-l})]$ in (21) can be alternatively represented as

$$\mathcal{Q}_l[\gamma(\mathbf{x}_{k-1} + s_{k-1}2^{-l})] = \gamma(\mathbf{x}_{k-1} + s_{k-1}2^{-l}). \quad (23)$$

That is, the quantization operation has no effect on $\gamma(\mathbf{x}_{k-1} + s_{k-1}2^{-l})$. This is because the vector s_{k-1} essentially captures the 1-bit quantization loss of $\mathcal{Q}_l[\gamma\mathbf{x}_{k-1}]$ per element.

Suppose in each forward pass in the training process, all the side information $\{s_{k-1}\}_{k=1}^{N-1}$ are stored in the memory. When we perform online back-propagation, each \mathbf{x}_{k-1} can be reconstructed losslessly in the form of

$$\mathbf{x}_{k-1} = \frac{1}{\gamma}\mathbf{x}_{k+1} - s_{k-1}2^{-l} - \frac{1}{\gamma}\mathcal{Q}_l[(1 - \gamma)\mathbf{x}_k + (1 + \gamma)\mathbf{h}_k(\mathbf{x}_k)] \quad k \geq 1. \quad (24)$$

Consequently, the computed gradient in the online back-propagation will not be drifted from the ground truth, which is desirable in very deep transformer models.

5 Experiments

We evaluated the BDIA training technique for both ViT-small by utilizing the open-source repository,² and nano-GPT2 by using the repository.³ It is found that the BDIA training technique produces promising performance in both tasks.

5.1 On training ViT-small

In this experiment, we consider training ViT-small over CIFAR10. When implementing the BDIA-training technique, the γ parameter was drawn from $\{-0.5, 0.5\}$ with equal probability per training sample per transformer block. The hyper-parameter l for quantization was set to $l = 9$. In addition, we utilize the SET-Adam optimizer [25] in the training process with the configuration $(\eta_0, \beta_1, \beta_2, \epsilon) = (1e - 4, 0.9, 0.999, 1e^{-18})$, where η_0 denotes the initial learning rate. The remaining training setups follow directly from the original open source. Three experimental repetitions were performed per training setup to mitigate the effect of randomness.

²<https://github.com/kentaroy47/vision-transformers-cifar10>

³<https://github.com/karpathy/nanoGPT>

Table 1 summarizes the obtained validation accuracy. It is clear that ViT-small with the BDIA training technique produces considerably better performance than without using BDIA. Fig. 2 visualize the training and validation curves. It is seen that even though the training loss when using the BDIA training technique is higher, the validation loss improves remarkably. This indicates that the random γ variable in BDIA indeed regularizes the ViT-small network properly.

Table 1: Validation accuracy for training ViT-small over CIFAR10

ViT-small	ViT-small with BDIA training
88.15 ± 0.55	89.10 ± 0.38

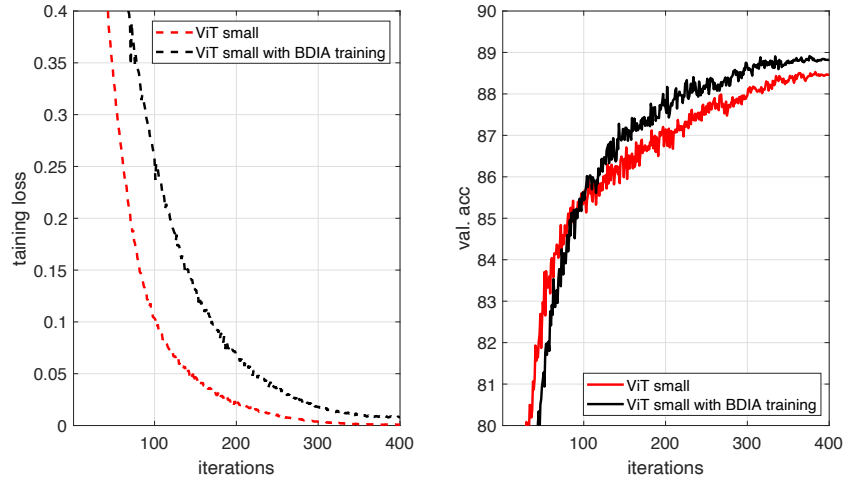


Figure 2: Performance comparison when training ViT small.

5.2 On training nano-GPT2

In this experiment, we consider training nano-GPT2 over the dataset of openwebtext. For illustration purpose, we only took a small subset from the entire training dataset when training the model. The parameter l for quantization was set to $l = 6$.

Fig. 3 summarizes the training and validation curves for three different training configurations. It is clear from the figure that the BDIA training technique makes the training procedure slightly slower. On the other hand, the resulting validation curve with BDIA is slightly better than without BDIA. The above results are consistent with those of Fig. 2 for training ViT-small.

Another interesting property in Fig. 3 is that GPT2 with and without quantization have very similar training and validation performance. That is, the impact of activation quantization in terms of performance is negligible.

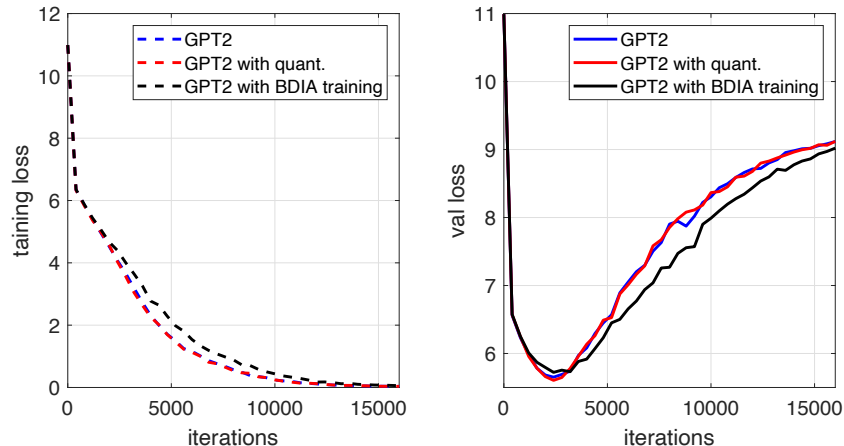


Figure 3: Performance comparison when training GPT2.

6 Conclusions

In this work, we have proposed the BDIA training technique to assist the training procedure of transformers. In particular, BDIA attempts to average every two consecutive integration approximations as a regularizer via the random variable $\gamma \in \{0.5, -0.5\}$. Exact bit-level reversibility for lossless online back-propagation can be achieved by performing activation quantization and storing lightweight side information. Experiments on training ViT-small and nano-GPT2 show that BDIA leads to better validation performance.

References

- [1] J. Achiam, S. Adler, S. Agarwal, F. L. A. Lama Ahmad, Ilge Akkaya, D. Almeida, J. Al-tenschmidt, S. Altman, S. Anadkat, R. Avila, I. Babuschkin, S. Balaji, V. Balcom, P. Baltescu, H. Bao, M. Bavarian, J. Belgum, I. Bello, J. Berdine, G. Bernadett-Shapiro, L. B. Christopher Berner, O. Boiko, M. Boyd, A.-L. Brakman, G. Brockman, T. Brooks, M. Brundage, K. Button, T. Cai, R. Campbell, A. Cann, B. Carey, C. Carlson, R. Carmichael, B. Chan, C. Chang, F. Chantzis, D. Chen, S. Chen, R. Chen, J. Chen, M. Chen, B. Chess, C. Cho, C. Chu, H. W. Chung, D. Cummings, J. Currier, Y. Dai, C. Decareaux, T. Degry, N. Deutsch, D. Deville, A. Dhar, D. Dohan, S. Dowling, S. Dunning, A. Ecoffet, A. Eleti, T. Eloundou, D. Farhi, L. Fedus, N. Felix, S. P. Fishman, J. Forte, I. Fulford, L. Gao, E. Georges, C. Gibson, V. Goel, T. Gogineni, G. Goh, R. Gontijo-Lopes, J. Gordon, M. Grafstein, S. Gray, R. Greene, J. Gross, S. S. Gu, Y. Guo, C. Hallacy, J. Han, J. Harris, Y. He, M. Heaton, J. Heidecke, C. Hesse, A. Hickey, W. Hickey, P. Hoeschele, B. Houghton, K. Hsu, S. Hu, X. Hu, J. Huizinga, S. Jain, and S. Jain. Gpt-4 technical report. arXiv:2307.09288 [cs.CL], 2023.
- [2] J. Behrmann, W. Grathwohl, R. T. Q. Chen, D. Duvenaud, and J.-H. Jacobsen. Invertible Residual Networks. In *Proceedings of the International Conference on Machine Learning (ICML)*, 2019.
- [3] B. Chang, L. Meng, E. Haber, L. Ruthotto, D. Begert, and E. Holtham. Reversible Architectures for Arbitrarily Deep Residual Neural Networks. arXiv:1709.03698v2 [cs.CV], 2017.
- [4] R. T. Q. Chen, Y. Rubanova, J. Bettencourt, and D. Duvenaud. Neural ordinary differential equations. In *32nd Conference on Neural Information Processing Systems (Neurips)*, 2018.
- [5] L. Dinh, D. Krueger, and Y. Bengio. Nice: Non-linear independent components estimation. arXiv preprint arXiv:1410.8516, 2014.
- [6] L. Dinh, J. Sohl-Dickstein, and S. Bengio. Density estimation using real nvp. arXiv preprint arXiv:1605.08803, 2016.
- [7] M. Finzi, P. Izmailov, W. Maddox, P. Kirichenko, and A. G. Wilson. Invertible convolutional networks. In *Workshop on Invertible Neural Nets and Normalizing Flows*, 2019.
- [8] A. Gholami, Z. Yao, S. Kim, M. W. Mahoney, and K. Keutzer. Ai and memory wall, 2021.
- [9] A. N. Gomez, M. Ren, R. Urtasun, and R. B. Grosse. The reversible residual network: Back-propagation without storing activations. arXiv:1707.04585v1 [cs.CV], 2017.
- [10] W. Grathwohl, I. S. R. T. Q. Chen, J. Bettencourt, and D. Duvenaud. Ffjord: Free-form continuous dynamics for scalable reversible generative models. arXiv:1810.01367, 2018.
- [11] T. Hascoet, Q. Fevre, Y. A. W. Zhuang, and T. Takiguchi. Layer-wise invertibility for extreme memory cost reduction of cnn training. In *Proceedings of the IEEE/CVF International Conference on Computer Vision Workshops*, 2019.
- [12] J.-H. Jacobsen, A. Smeulders, and E. Oyallon. i-revnet deep invertible networks. In *ICLR*, 2018.
- [13] D. P. Kingma and P. Dhariwal. Glow: Generative flow with invertible 1x1 convolutions. In *Advances in neural information processing systems*, 2018.
- [14] I. Kobyzev, S. J. Prince, and M. A. Brubaker. Normalizing Flows: An Introduction and Review of Current Methods. *PAMI*, (11):3964–3979, 2020.

- [15] K. Mangalam, H. F. adn Y. Li, C.-Y. Qu, B. Xiong, C. Feichtenhofer, and J. Malik. Reversible vision transformers. arXiv:2302.04869v1 [cs.CV], 2023.
- [16] M. E. Sander, M. B. P. Ablin, and G. Peyre. Momentum residual neural networks. arXiv:2102.07870, 2021.
- [17] J. Song, C. Meng, and S. Ermon. Denoising Diffusion Implicit Models. In *ICLR*, 2021.
- [18] Y. Song, C. Meng, and S. Ermon. Mintnet: Building invertible neural networks with masked convolutions. arXiv:1907.07945, 2019.
- [19] J. Stam. An exact bitwise reversible integrator. arXiv:2207.07695 [cs.GR], 2022.
- [20] H. Touvron, L. Martin, P. A. K. Stone, A. Almahairi, Y. Babaei, N. Bashlykov, S. Batra, P. Bhargava, S. Bhosale, D. Bikel, L. Blecher, C. C. Ferrer, M. Chen, G. Cucurull, D. Esiobu, J. Fernandes, J. Fu, W. Fu, B. Fuller, C. Gao, V. Goswami, N. Goyal, A. Hartshorn, S. Hosseini, R. Hou, H. Inan, M. Kardas, V. Kerkez, M. Khabsa, I. Kloumann, A. Korenev, P. S. Koura, M.-A. Lachaux, T. Lavril, J. Lee, Y. L. Diana Liskovich, Y. Mao, X. Martinet, T. Mihaylov, P. Mishra, I. Molybog, A. P. Yixin Nie, J. Reizenstein, R. Rungta, K. Saladi, A. Schelten, R. Silva, E. M. Smith, R. Subramanian, X. E. Tan, B. Tang, R. Taylor, J. X. K. Adina Williams, P. Xu, Z. Yan, I. Zarov, Y. Zhang, A. Fan, M. Kambadur, A. R. Sharan Narang, R. Stojnic, S. Edunov, and T. Scialom. Llama 2: Open foundation and fine-tuned chat models. arXiv:2307.09288 [cs.CL], 2023.
- [21] B. Wallace, A. Gokul, S. Ermon, and N. Naik. End-to-End Diffusion Latent Optimization Improves Classifier Guidance. arXiv:2303.13703v2 [cs.CV], 2023.
- [22] N. Wang, J. Choi, D. Brand, C.-Y. Chen, and K. Gopalakrishnan. Training deep neural networks with 8-bit floating point numbers. In *NeurIPS*, 2018.
- [23] S. Wu, G. Li, F. Chen, and L. Shi. Training and inference with integers in deep neural networks. In *ICLR*, 2018.
- [24] G. Yang, T. Zhang, P. Kirichenko, J. Bai, A. G. Wilson, and C. D. Sa. SWALP: Stochastic Weight Averaging in Low-Precision Training. In *ICML*, 2019.
- [25] G. Zhang. On Suppressing Range of Adaptive Stepsizes of Adam to Improve Generalisation Performance. 2024.
- [26] G. Zhang, J. P. Lewis, and W. B. Kleijn. Exact diffusion inversion via bidirectional integration approximation. arXiv:2307.10829 [cs.CV], 2023.
- [27] G. Zhang, K. Niwa, and W. B. Kleijn. On Accelerating Diffusion-Based Sampling Processes by Improved Integration Approximation. arXiv:2304.11328 [cs.LG], 2023.
- [28] T. Zhu and K. Mangalam. Pareprop: Fast parallelized reversible backpropagation. arXiv:2306.09342v1 [cs.LG], 2023.